Nonlinear Dyn (2016) 86:1841–1854
DOI 10.1007/s11071-016-2996-6

ORIGINAL PAPER

The investigation of chemical coupling in a HR neuron model with reconfigurable implementations

Nimet Korkmaz · İsmail Öztürk · Recai Kılıç

Received: 8 April 2016 / Accepted: 30 July 2016 / Published online: 9 August 2016

Abstract Although there are a lot of studies on realization of electrical coupling in HR neuron model, the investigation of chemical coupling with hardware implementations is limited because of implementation complexities. In this paper, it is aimed to present alternative analog and digital hardware solutions for investigating the chemical coupling in the HR neuron model. In order to implement the chemical coupled HR neuronal system on a reconfigurable digital platform, chemical coupling function is modified, and the stability control of the new modified chemical coupling function is checked by using the standard deviation method. Simple artificial network structure using two chemical coupled HR neurons reminds of the small part of the stomatogastric ganglion central pattern generator (CPG) circuit of a lobster. Thus, a simple CPG structure is also realized electronically and asynchronous behaviors between the chemical coupled neurons in this CPG are emulated successfully by using these programmable analog and digital devices.

N. Korkmaz (✉) · İ. Öztürk · R. Kılıç
Department of Electrical and Electronic Engineering, Erciyes University, 38039 Kayseri, Turkey
e-mail: nimetdahasert@erciyes.edu.tr

İ. Öztürk
e-mail: ismailozturk@erciyes.edu.tr

R. Kılıç
e-mail: kilic@erciyes.edu.tr

Keywords Hindmarsh–Rose neuron model · Synchronization · Chemical coupling · FPAA · FPGA · Central patten generators (CPGs)

1 Introduction

Synchronization of the nonlinear oscillators is an often-studied issue by many researchers interested in dynamical system theory, and the synchronization of the neurons has been also a trend topic in this area in order to play an important role in information processing of the brain recently [1–7]. Neurons can produce own inherent electrical potentials via the ion flows through the surface of membrane, and these inherent membrane oscillations are modeled with the several biological neuron models such as Hodgkin–Huxley (HH), FitzHugh–Nagumo (FHN), Wilson–Cowan (WC), Morris–Lecar (ML), Hindmarsh–Rose(HR) and Izhikevich (IZ) like a nonlinear oscillator [8–13]. There are advantages and disadvantages of each of these biological neuron models. For example, HH neuron model discusses the ionic mechanism and electrical current on membrane surface comprehensively, but this model is not preferred in some applications because of the calculation complexities [8]. FHN neuron model is the simplified type of the HH neuron model in terms of the calculation easiness, but bursting behaviors of the neurons cannot be obtained with this model [9]. On the other hand, HR neuron model is derived from the FHN neuron model

and a lot of dynamical behaviors of the neurons can be observed via this model [12].

In addition to model the dynamical individual behaviors of the neurons, the synchronization situations of the collective neurons are also obtained physically via the biological neuron models. Since it is very difficult to identify the interaction of the collective neurons in the living body, the interactions between the neurons can be modeled by coupling the biological neuron models. In the literature, the studies examining the neuronal synchronization are generally performed by the HR neuron model due to its definition and calculation simplicity. In these synchronization studies performed using the HR neuron model, a few issues are handled like that: *Coupling type*: synaptic connections of the neurons are either chemical or electrical, and they are defined by the mathematical functions separately [14]. These coupling types are adapted to the HR neuron model, and the studies examined the effects on the synchronization status of coupling types are reported in the literature [15–18]. *Control of the synchronization*: synchronization refers to the closeness of the frequency or phase of two systems that generate periodic or chaotic oscillations. The synchronization status of the coupled HR neurons can be controlled in various ways such as nonlinear feedback control, backstepping control, active control, H_∞ variable universe adaptive fuzzy control, and adaptive sliding mode control [19–28]. *Stability control approaches in synchronization*: in the literature, after the dynamical nonlinear systems are synchronized using the control methods, various stability control approaches such as master stability function method, the connection graph stability method, the linear matrix inequality approach, matrix measure approach, the eigenvalue approach, and standard deviation method are used to check the achievement of the synchronization process [29–46]. *Adapting the data from a real neuron to biological model*: after the processing the obtained data from living cells, it is tried to adapt these results to the biological neuron model in some studies. In contrast to this type study, the response of a real nerve is sometimes controlled by utilizing the simulation results of the biological neuron model [47–50]. *The usage of the neuron models in the practical applications*: biological neuron models are implemented with the several electronic devices for some applications that require real-time signals and artificial neurons are obtained electronically [51–58].

In the literature, although there are a lot of studies on realizing a single neuron with several electronic devices [51–58], the number of the studies coupled artificial neurons electronically or electronic applications of synchronization studies are limited because of implementation complexities [53,59–65]. However, electrical coupling is usually preferred in these available hardware implementation studies because of mathematical description simplicity. In our previous study, the experimental realizations of HR neuron model with programmable hardware and synchronization applications via electrical coupling have been investigated [61]. On the other hand, several CMOS or analog realization studies utilizing the characteristics of analog devices are offered [51–64]. Other neuron models, which cannot model the electrical and chemical coupling separately, are used as an example of chemical coupling application [63,65]. However, no study about the digital implementation of chemical coupling defined by a complex nonlinear function in HR neurons is reported in the literature to the best of our knowledge.

In this study, after two HR neurons are connected with the chemical coupling function, this chemical coupled simple artificial network is implemented with reconfigurable analog and digital devices. For the digital implementation easiness, chemical coupling function is modified, and the stability control of the new modified chemical coupling function is checked by using the standard deviation method. Furthermore, this HR neuron model based and chemical coupled simple artificial network structure reminds of the small part of the stomatogastric ganglion central pattern generator (CPG) circuit of a lobster because synaptic connections between pyloric dilator (PD) and lateral pyloric (LP) neurons are chemical and unidirectional [66]. These two neurons exhibit asynchronous behaviors. Here, PD and LP neurons in this CPG circuit are represented by two HR neurons and synaptic connections are modeled via new modified chemical coupling and asynchronous behaviors can be obtained by adjusting synaptic weights in the chemical coupling functions. The results of the standard derivative method are used to adjust the synaptic weights, so asynchronous behaviors between two neurons are obtained easily. As results of these studies, not only chemical coupling function in HR neurons is implemented with digital devices for the first time but also a simple CPG structure is realized electronically by using programmable analog and digital devices.

Neuron coupling types, HR neuron model, coupling of the HR neurons, and the stomatogastric ganglion central pattern generator (CPG) circuit of a lobster are briefly handled in Sect. 2. In this section, after the modified chemical coupling function is introduced, numerical simulation results and the results of standard deviation methods for original and modified chemical coupling are also given together to see the closeness of the nonlinear function characteristics and to examine the synchronization situations of the chemical coupled HR neurons. The details of programmable analog and digital devices-based realizations of chemical coupled HR neurons, namely simple CPG circuit applications, are given in Sect. 3. Some concluding remarks and comparisons are presented in the last section.

2 Chemical coupling of HR neurons

The co-ordination between neurons occurs via their synaptic connections. There are two type synaptic connections including electrical and chemical [14–18]. An electrical coupling is a mechanical and electrically conductive link between two neurons. It is formed at a narrow gap between the pre- and postsynaptic cells known as a gap junction. If the voltage of one neuron changes, ions may move through from one cell to the next, so the ions of two neurons flow in direct proportion to the difference between the membrane potential of the neurons. Since electrical coupling can cause either neuron to influence the other, these are bidirectional synapses. On the other hand, there is a gap junction between two neurons in the chemical coupling and the space between the chemical couplings is much larger than an electrical ones. Thus, electrical coupling is faster than the chemical one. In the chemical coupling, the presynaptic neuron releases a chemical (a neurotransmitter) which rapidly crosses the small space across the synapse and binds to a receptor on the postsynaptic neuron. After the neurotransmitter enzymes are released between two neurons, action potential forms in the postsynaptic neuron. If the realized enzyme facilitates the action potential generation, this type chemical coupling is named excitatory coupling; else inhibitory coupling occurs between the two neurons. The difference between an electrical and chemical coupling is the conduction methods between the neurons, but one is not more important than another. They serve different purposes. The one of the most successful neuron models is HR neuron model reflecting these properties of the neurons and synaptic connections. Electrical and chemical coupling can be modeled separately by using HR neuron model, and this is the most important advantage of the coupled HR neurons. FHN and HR neuron models are the simplified type of the Hodgkin–Huxley neuron model. While FHN neuron model does not exhibit some neuron dynamics such as bursting behavior, several dynamic behaviors of a real neuron can be observed with HR neuron model derived from the FHN neuron models. HR neuron model is defined by the following differential equations [12]:

$$\begin{aligned}\dot{x} &= f_x(x, y, z) = y - x^3 + bx^2 + I - z\\ \dot{y} &= f_y(x, y, z) = 1 - 5x^2 - y\\ \dot{z} &= f_z(x, y, z) = \mu(s(x - x_{\text{rest}}) - z)\end{aligned} \tag{1}$$

where I represents the membrane input current, b controls the transition between bursting and spiking, μ controls the spiking frequency and the number of spikes per burst in the case of spiking and bursting respectively, s adjusts adaptation, x_{rest} is the resting potential. After the parameters $\mu = 0.01$, $s = 4$, $x_{\text{rest}} = -1.6$ are fixed, several different dynamical behaviors of HR neuron model can be obtained by adjusting the b and I parameters. While $b = 2.96$, $I = 5$ are set to observe the spiking behavior as shown in Fig. 1a, the bursting behavior in Fig. 1b is obtained for the parameter values of $b = 2.6$, $I = 2.22$.

Several studies on synchronization and coupling of the two HR neurons have been reported in the literature. The two coupled HR neurons can be defined by the following equations [46]:

$$\begin{aligned}\dot{x}_1 &= f_x(x_1, y_1, z_1) - g_s\delta(x_1)\breve{c}_{12}\gamma(x_1, x_2)\\ \dot{y}_1 &= f_y(x_1, y_1, z_1)\\ \dot{z}_1 &= f_z(x_1, y_1, z_1)\\ \dot{x}_2 &= f_x(x_2, y_2, z_2) - g_s\delta(x_2)\breve{c}_{21}\gamma(x_2, x_1)\\ \dot{y}_2 &= f_y(x_2, y_2, z_2)\\ \dot{z}_2 &= f_z(x_2, y_2, z_2)\end{aligned} \tag{2}$$

where $\breve{c}_{12} = \breve{c}_{21} = 1$. The parameter (g_s) in Eq. 2 is known as the strength of coupling. In case of the chemical coupling, for the first neuron $\gamma(x_1, x_2) = \gamma_c(x_2) = (1/(1 + e^{-k(x_2-\theta_s)}))$, $\delta(x_1) = -(x_1 - V_s)$ and for the second neuron, $\gamma(x_2, x_1) = \gamma_c(x_1) = (1/(1 + e^{-k(x_1-\theta_s)}))$, $\delta(x_2) = -(x_2 - V_s)$. Two neurons with chemical coupling were simulated according to $k = 10$, $V_s = -2$, $\theta_s = -0.28$ by using a simulation model in Eq. 2 where no control method is applied. The

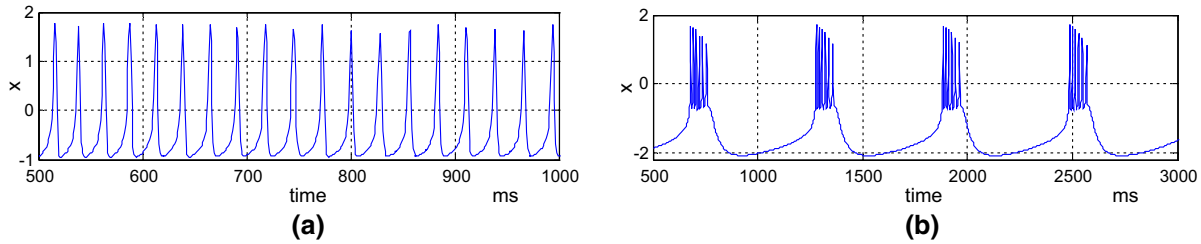

Fig. 1 HR neuron dynamics for **a** spiking mode, **b** bursting mode

synchronization situation of the neurons is impressed by the value of (g_s) parameter both in electrical and chemical coupling. As mentioned before, various stability control approaches have been proposed to control the synchronal situations between the neurons and one of them is standard deviation method described by Eq. 3 [31]:

$$\sigma = [\langle \sigma(k) \rangle]$$
$$\sigma(k) = \sqrt{\frac{\left[\frac{1}{N}\sum_{i=1}^{N} x_i^2(k) - \left[\frac{1}{N}\sum_{i=1}^{N} x_i(k)\right]^2\right]}{(N-1)}} \quad (3)$$

where $\sigma\ (k)$ is the kth value in the time series of the kth neuron, $\langle * \rangle$ denotes the average value of $\sigma\ (k)$ over the evolution time, and [*] denotes the value of σ. This method means that for the synchronal two HR neurons: As the dynamical behaviors of two HR neurons get close to each other, the results of the standard deviation function converges to zero. According to the standard deviation graph calculated for chemical coupled two HR neurons in Fig. 2a, chemical coupled two HR neurons exhibit asynchronous, partially synchronous and synchronous behaviors for $g_s = -2$, $g_s = 0.6$, $g_s = 5$, respectively. The phase portrait illustrations of the chemical coupled two HR neurons with these synaptic weights are given, respectively, in Fig. 2b–d. In these figures, x_1 and x_2 represent the membrane potentials of the first and second neurons. The numerical simulation results in these figures verify the results of the standard deviation methods.

Exponential function in chemical coupling description is hard to implement with the digital platforms, so this description must be predisposed to digital realizations. A new approximate function in Eq. 4 is proposed for implementation easiness:

$$\gamma(x) = \frac{1}{1+e^{-2kx}} \cong \frac{1}{2} + \frac{1}{2}\tanh(kx)$$
$$\tanh(kx) \cong \frac{kx}{\sqrt{1+kx^2}} \cong \frac{kx}{1+|kx|}$$
$$\gamma(x) = \frac{1}{1+e^{-2kx}} \cong \frac{1}{2} + \frac{1}{2}\left(\frac{kx}{1+|kx|}\right) \quad (4)$$

where $k = 10$. Figure 3 shows the closeness between original and modified chemical coupling functions. In this figure, while the continuous line is the original chemical function characteristic, the nonlinear characteristic of the modified function in Eq. 4 is given with the dotted line.

Using of the similarity of these two nonlinear functions, two HR neurons are coupled with modified coupling function. For the purpose of identifying the synchronous statuses of these two HR neurons, standard deviation calculation is repeated for modified chemical coupled HR neurons and the results of this calculation are given in the Fig. 4a. Two results in Figs. 2a and 4a are very similar each other. The numerical simulation results for asynchronous, partially synchronous and synchronous behaviors of the modified chemical coupled two HR neurons are given in Fig. 4b–d, respectively, and the modified chemical coupling weights are adjusted to $g_s = -2$, $g_s = 0.6$, $g_s = 5$ in these numerical simulations. In whole numerical simulations, Euler discretization methods has been used by taking the discretization constant as $\Delta h = 0.01$ and the initial conditions as $(x_1(0), y_1(0), z_1(0)) = (1, 0, 0)$ and $(x_2(0), y_2(0), z_2(0)) = (2, 0, 0)$, respectively. Additionally, the model parameter values of HR neurons in the chemical and modified chemical coupled structures are adjusted to same values with the bursting behavior of HR neuron model in Fig 1b, namely, $\mu = 0.01$, $s = 4$, $x_{\text{rest}} = -1.6$, $b = 2.6$, $I = 2.22$.

In order to investigate the coupling types and synchronization situations between neurons, the central pattern generators (CPGs) networks are the suitable

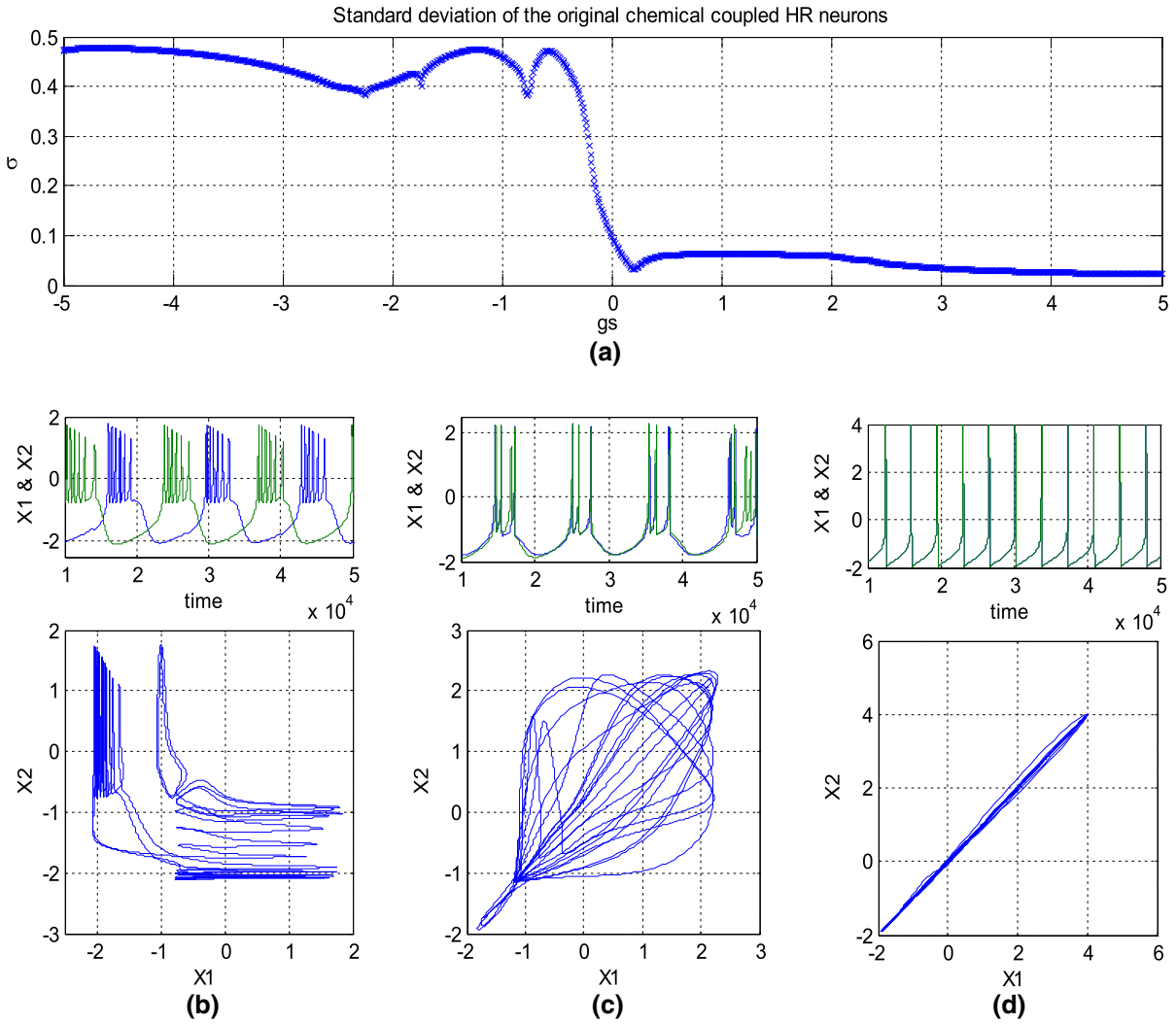

Fig. 2 **a** Standard deviation graph of the chemical coupled two HR neurons for the synchronization stability. Time series and phase portrait illustrations of the chemical coupled two HR neurons for $b = 2.6, I = 2.22$, **b** asynchronous behaviors for $g_s = -2$, **c** partially synchronous behaviors for $g_s = 0.6$, **d** synchronous behaviors for $g_s = 5$

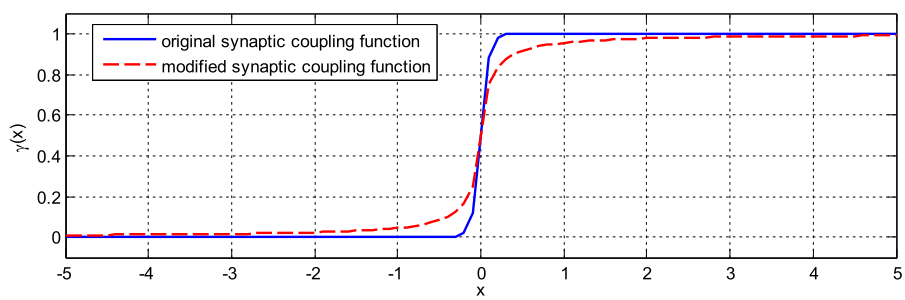

Fig. 3 Nonlinear characteristics of the original and modified chemical coupling functions

structures. Central pattern generators are the specific neural networks which can produce a coordinated rhythmic activity pattern without any rhythmic introduction from the high control centers or sensor feedback in the living body [67]. The neurons in these networks communicate with each other through electri-

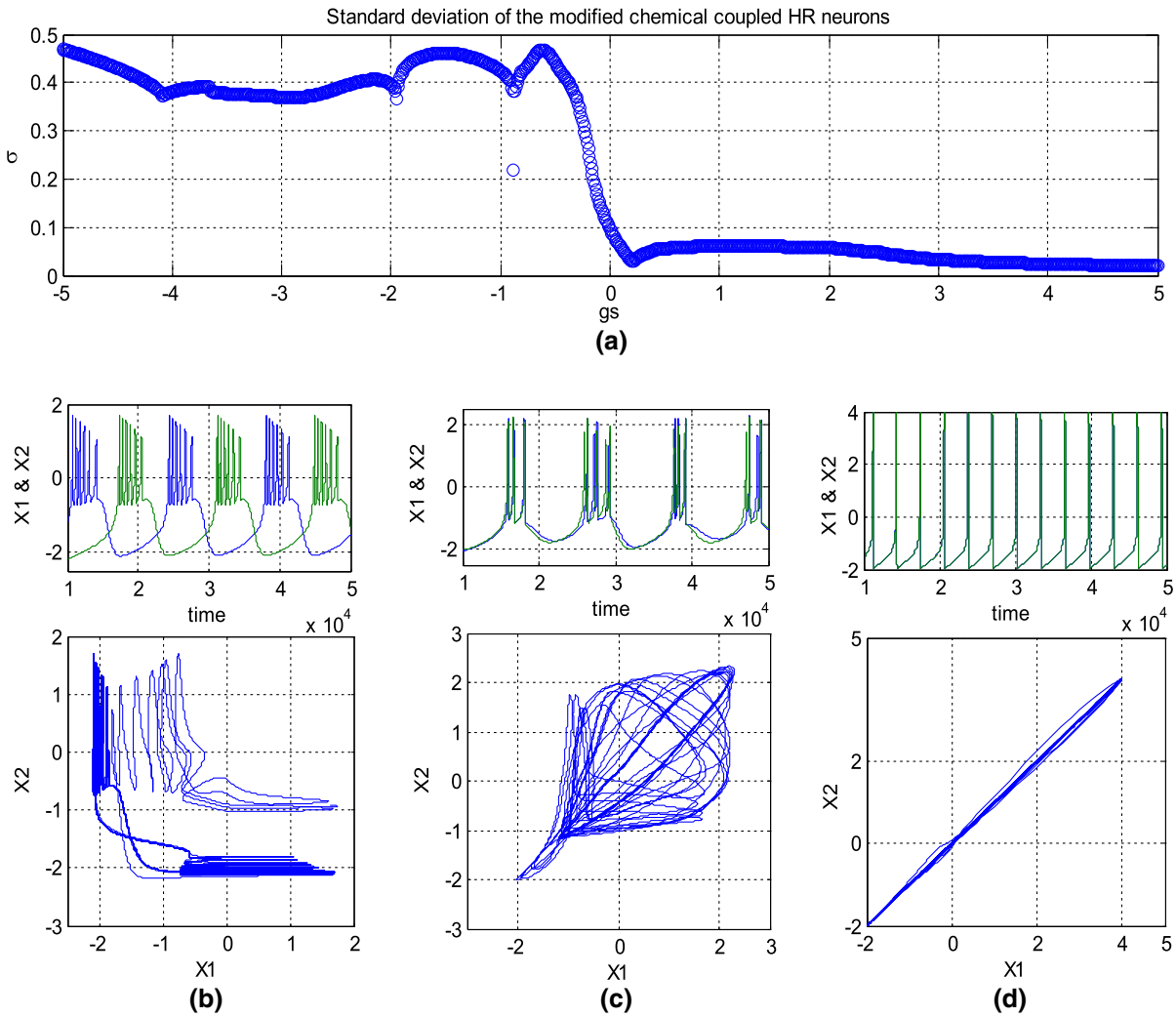

Fig. 4 **a** Standard deviation graph of the modified chemical coupled two HR neurons for the synchronization stability. Time series and phase portrait illustrations of the chemical coupled two HR neurons for $b = 2.6$, $I = 2.22$, **b** asynchronous behaviors for $g_s = -2$, **c** partially synchronous behaviors for $g_s = 0.6$, **d** synchronous behaviors for $g_s = 5$

cal coupling and chemical coupling, and CPG network structures can be modeled with biological neuron models. In a CPG structure, a rhythmic motor pattern is generated by a pacemaker neuron that can serve as a source of the rhythm. The phase relationships and frequency of the rhythms are based on the network interactions and sensory and central modulation. The pyloric rhythm of a lobster is one of the best understood CPG circuits, and this CPG circuit is given in Fig. 5a. The pyloric rhythm consists of a five-phase rhythm as seen in Fig. 5b. The core of the rhythm is a repeating cycle of activity in which the lateral pyloric (LP), pyloric (PY) and pyloric dilator (PD) neurons fire sequentially. The inferior cardiac (IC) fires in LP time, and the ventricular dilator (VD) often fires in PY time. The AB neuron is the one interneuron of this CPG network and fires in time with the PD neurons. Additionally, PD and LP neurons exhibit asynchronous behavior as seen in Fig. 5b [66]. Here, the asynchronous behaviors of PD and LP neurons are focused. Thus, phase differences between the neurons have been considered rather than the dynamical behaviors of neurons. PD and LP neurons in this CPG network are represented by two HR neurons. Synaptic connections are modeled via new modified chemical coupling, and asynchronous behaviors can be obtained by adjusting the chemical coupling weight to

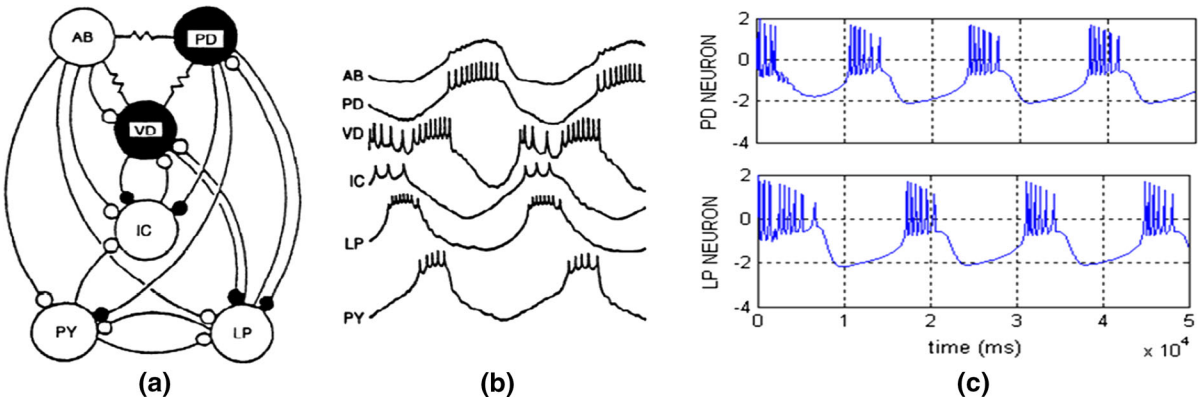

Fig. 5 **a** Pyloric stomatogastric CPG network of a lobster (coupled PD and LP neurons), **b** the dynamical behaviors of the neurons in the pyloric stomatogastric CPG network [66], **c** numerical simulation results of modified chemical coupled two HR neurons for $g_s = -2$

$g_s = -2$ according to the results of the standard deviation calculation in Fig. 4. Numerical simulation results in Fig. 5c of modified chemical coupled two HR neurons for $g_s = -2$ illustrate this asynchronous behaviors. As it is seen from these results, the neurons and synaptic connections in a CPG network can be modeled with HR biological neuron model successfully.

3 Hardware implementations of the chemical coupled two HR neurons

Biological neuron models, coupled artificial neurons and CPG networks, can be implemented with various devices for the some applications required real-time signals. Here, the design processes of programmable analog device- and digital device-based the chemical coupled two HR neurons are presented in detail. Since this chemical coupled simple network reminds of the small part of the stomatogastric ganglion CPG circuit of a lobster, asynchronous behaviors of chemical coupled HR neurons are presented as the results of the experimental realizations. Namely, the programmable analog device- and digital device-based implementations of the chemical coupled PD and LP neurons which are modeled by HR neuron model are presented in this section.

3.1 Programmable analog device-based implementation

Several studies about analog devices-based realizations of HR neuron model and the coupled HR neurons have been reported in the literature [51–60], and the experimental realizations of a HR neuron and the electrical coupled HR neurons with programmable analog device are also presented in literature by us [61]. However, any realization example of the chemical coupled HR neurons with a programmable and reconfigurable platform has not been recommended yet. To emulate the interaction of the collective neurons faultlessly and to operate bio-inspired structures precisely, this shortcoming about realization with programmable analog device must be addressed as well. Thus, the realization details of the chemical coupled HR neurons with FPAA (field programmable analog array) are given in this part.

FPAA (field programmable analog array) is a very useful experimental platform with its high stability, accuracy and rapid prototyping specialties to investigate neuronal structures. This programmable analog device is based on the switched-capacitor technology, and it has some limitations such as capacity and a specific saturation level, (± 2 V). However, FPAA boards can be combined with each other in order to cope with the capacity problem and the saturation problem is resolved with a rescaling operation. The predefined configurable analog modules (CAMs) in the software tool Anadigm Designer2 are used to implement analog functions such as multiplication, addition, filtering, rectification, etc. In this study, AN231E04 type FPAA boards was used and comprehensive descriptions of the CAMs are available on this software tool [68].

As seen from Fig. 6, four FPAA boards are used to implement two chemical coupled HR neurons. These

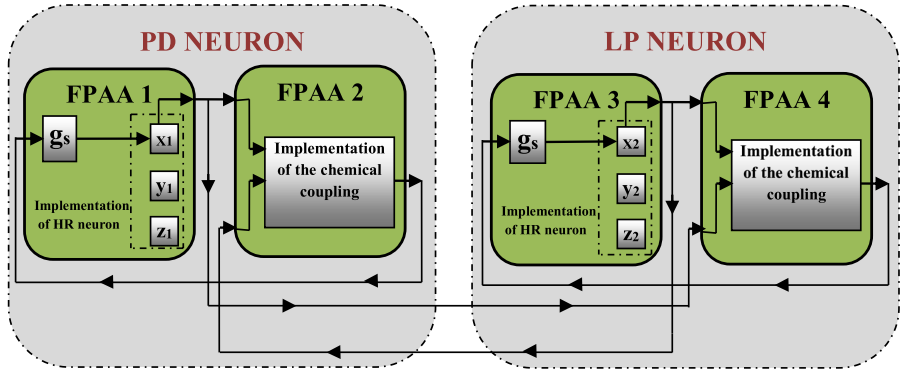

Fig. 6 **a** Schematic block diagram for FPAA-based implementation of chemical coupled two HR neurons

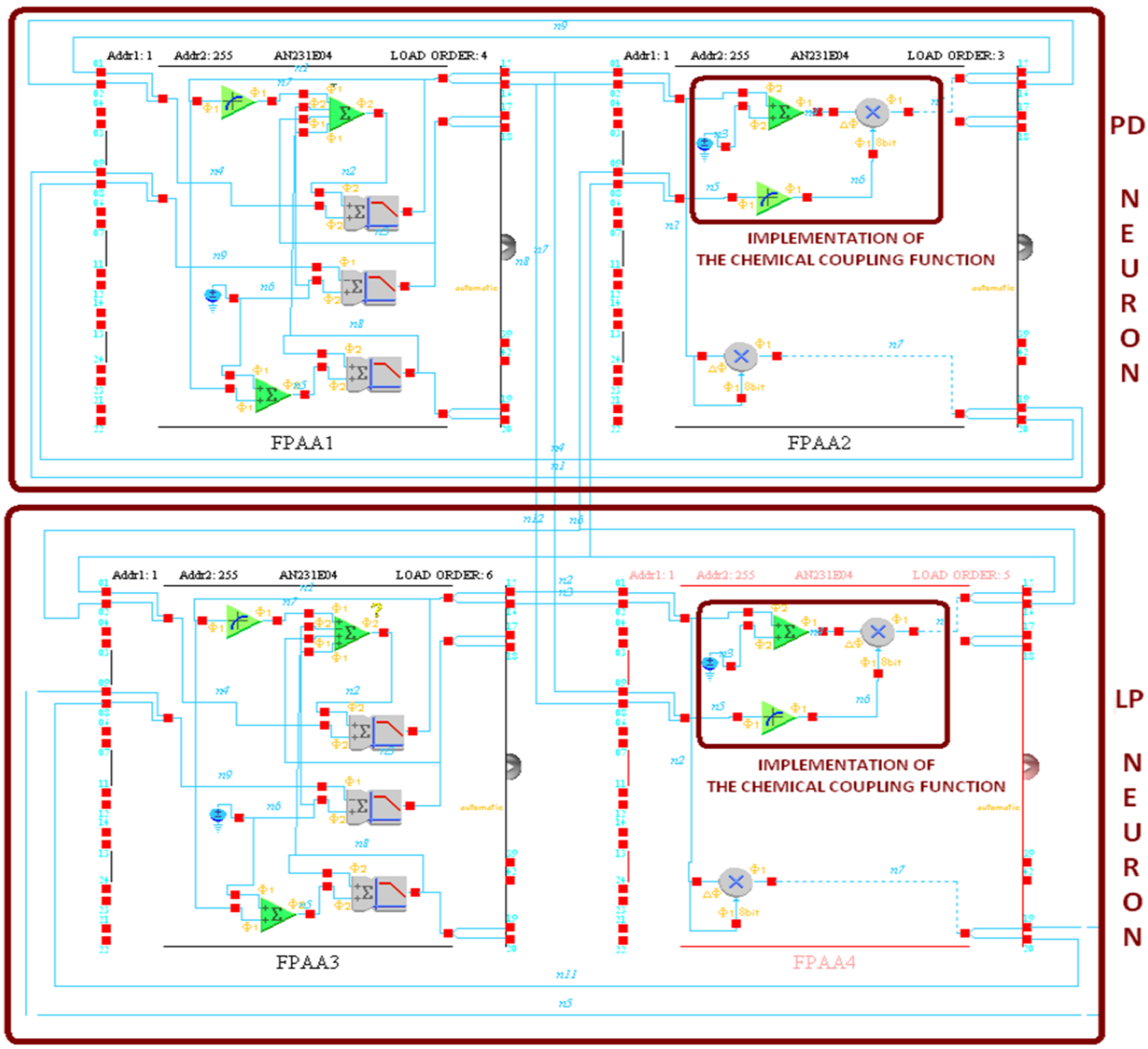

Fig. 7 FPAA implementation scheme of the chemical coupled HR neurons

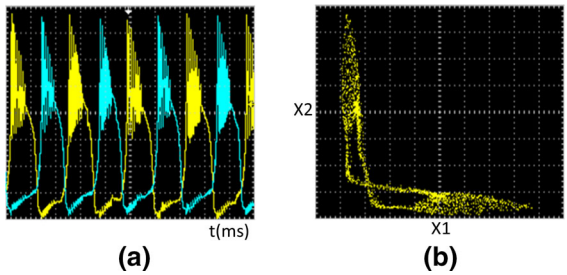

Fig. 8 FPAA-based experimental results of the chemical coupled two HR neurons for implementation easiness: x_1, x_2 time domain illustrations, x, 200 mV/div; y, 200 mV/div; time/div, 10 ms. **b** x-y phase portrait illustration of x_1 and x_2, x, 200 mV/div; y, 200 mV/div for asynchronous behavior

two HR neurons can be assumed PD and LP neurons in the stomatogastric CPG. While PD neuron is contracted with FPAA1&2 boards, LP neuron is embedded FPAA3&4.

PD and LP neurons represented by HR neuron model are implemented with FPAA as in Ref [61], and same parameter values in Ref [61] are also used in this study to implement HR neurons with FPAA. However, the realization of the chemical coupling is integrated to this study. The chemical coupling function for the first neuron is defined by $\gamma(x_1, x_2) = \gamma_c(x_2) = (1/(1 + e^{-k(x_2-\theta_s)}))$, $\sigma(x_1) = -(x_1 - V_s)$ functions. In the chemical coupling, $\gamma_c(x_j)$ functions are implemented by using TRANSFER FUNCTION blocks in the FPAA2&4 as seen in Fig. 7. $\sigma(x_i)$ function consists of a difference expression and this function is realized with a SUMDIFF block. V_s parameter in this difference expression is a constant value, and it is implemented with a VOLTAGE CAM block. Finally, the MULTIPLIER block is used for performing the multiplication operation in this synaptic connection. Synchronous situations between the chemical coupled HR neurons change depending on the (g_s) parameter, and this parameter can be adjusted with the gain of the MULTIPLIER block and it is adjusted to -0.5 after the rescaling process for asynchronous behavior. The experimental results of the asynchronous behavior between chemical coupled PD and LP neuron are given in Fig. 8 for the FPAA-based realization. The CAB usage capacities and power consumptions of chemical coupling implementations are given in Table 1. The performance of the electrical and chemical coupling can be considered both together and separately in the modeling and implementation studies. It is useful to present the differences

Table 1 Power consumptions and CAB usage capacity of the FPAA-based coupled neurons implementation

	Power consumption (mW)	CAB1 (used /total capacity)	CAB2 (used /total capacity)	CAB3 (used /total capacity)	CAB4 (used /total capacity)
Electrical coupling results [61]					
Neuron I					
FPAA 1	128 ± 38	8/8	7/8	5/8	5/8
FPAA 2	56 ± 17	7/8	0/8	0/8	0/8
Neuron II					
FPAA 3	128 ± 38	8/8	7/8	5/8	5/8
FPAA 4	56 ± 17	7/8	0/8	0/8	0/8
Chemical coupling results					
Neuron I					
FPAA 1	127 ± 38	8/8	8/8	4/8	5/8
FPAA 2	93 ± 28	7/8	5/8	4/8	0/8
Neuron II					
FPAA 3	127 ± 38	8/8	8/8	4/8	5/8
FPAA 4	93 ± 28	7/8	5/8	4/8	0/8

and similarities between the electrical and chemical coupling studies. In this context, the results of the electrical coupled implementation studies in Ref. [61] are given with the results of chemical ones comparatively in the both FPAA- and FPGA-based implementations. To compare the FPAA-based implementation results of electrical and chemical coupling in terms of area usage, power consumption and implementation advantages, the electrical coupling results coupling in Ref [61] are also given in Table 1. Since chemical coupling functions are constructed on the FPAA2 and FPAA4 boards, CAB usage capacities and power consumptions of these boards increase just a little according to these results. However, the nonlinear expression in the chemical coupling can be embedded only one CAB block and chemical coupling function is implemented easily with FPAA as the electrical coupling.

These experimental results match the numerical simulation result in Fig. 2. By changing the parameter (g_s), another synchronization status or realization studies can be implemented easily in this experimental platform without time consumption and another studies about neuron synchronization can be proved rapidly with this analog programmable and reconfigurable device.

3.2 Programmable digital device-based implementation

In the digital experimental realization studied, the models included electrical coupling function and simple descriptions are preferred for implementation easiness. No study about the digital implementation of the chemical coupling defined by a complex nonlinear function is reported in the literature. In this study, to overcome this implementation difficulty, exponential expression in the chemical coupling function are converted to an approximate nonlinear function which is more suitable for digital hardware implementation as mentioned in previous section. Here, the programmable digital device-based implementation of the chemical coupled two HR neurons is made by utilizing the approximate function in Eq. 4 and modified chemical coupled two HR neurons are implemented with FPGA (field programmable gate array) as an example of digital realization for the first time in literature.

In this FPGA-based implementation, it is handled using Cyclone III IC which has 15408 digital blocks and 112 embedded multipliers [69]. Since FPGA is a digital platform, implementation process requires discretization of differential equations in Eq. 1. Euler method is preferred for the discretization because of its simplicity, and the discretization constant is chosen as $\Delta h = 0.01$. Resulting discrete equations are seen in Eq. 5.

$$\begin{aligned} x_{n+1} &= x_n + \Delta h(y_n - x_n^3 + bx_n^2 + I - z_n) \\ y_{n+1} &= y_n + \Delta h(1 - 5x_n^2 - y_n) \\ z_{n+1} &= z_n + \Delta h(\mu(s(x_n - x_{\text{rest}}) - z_n)) \end{aligned} \tag{5}$$

The equation of the modified chemical coupling in Eq. (4) is used to couple two discretized neurons with the initial conditions: $(x_1(0), y_1(0), z_1(0)) = (1, 0, 0)$ and $(x_2(0), y_2(0), z_2(0)) = (2, 0, 0)$, respectively. Also, the model parameter values of modified chemical coupled HR neurons are adjusted to $\mu = 0.01$, $s = 4$, $x_{\text{rest}} = -1.6$, $b = 2.6$, $I = 2.22$ values. A block diagram of the FPGA-based implementation for chemical coupled two HR neurons is shown in Fig. 9a. These neurons and their synaptic coupling are defined using VHDL language as in Fig. 9b, and 24-bit fixed point arithmetic (Q7.16) is used in arithmetic operations. (x_n) values of each neuron are truncated into 8 bits in order to see their outputs using 8-bit D/A converters. Since the PD and LP neurons represented by HR neurons are handled in this study, the FPGA-based realization results of modified coupled HR neurons are given for asynchronous behavior for $g_s = -2$ in Fig. 10. However, the synchronization statuses of modified chemical coupled HR neurons are adjusted by depending on the values of (g_s).

The synthesis results of FPGA-based realization are given in Table 2, and they are compared with the electrical coupled HR neurons implementation in Ref. [61] in order to see trade-off of the FPGA-based implementations of the coupling methods in terms of area and multiplier usage and maximum frequency range. As it is seen, there is a drastic decrease in the maximum operating frequency when the synaptic coupling is used in implementation. Also, the area consumption is almost doubled. The main culprit behind this costly and slower result is the division operation which is required in the chemical coupling (Eq. 4). As the number of bits increases, digital implementation of a divider becomes costly and the operation becomes slower. Therefore, while digital implementation deficiency problem of the chemical coupled HR neurons is alleviated by using this

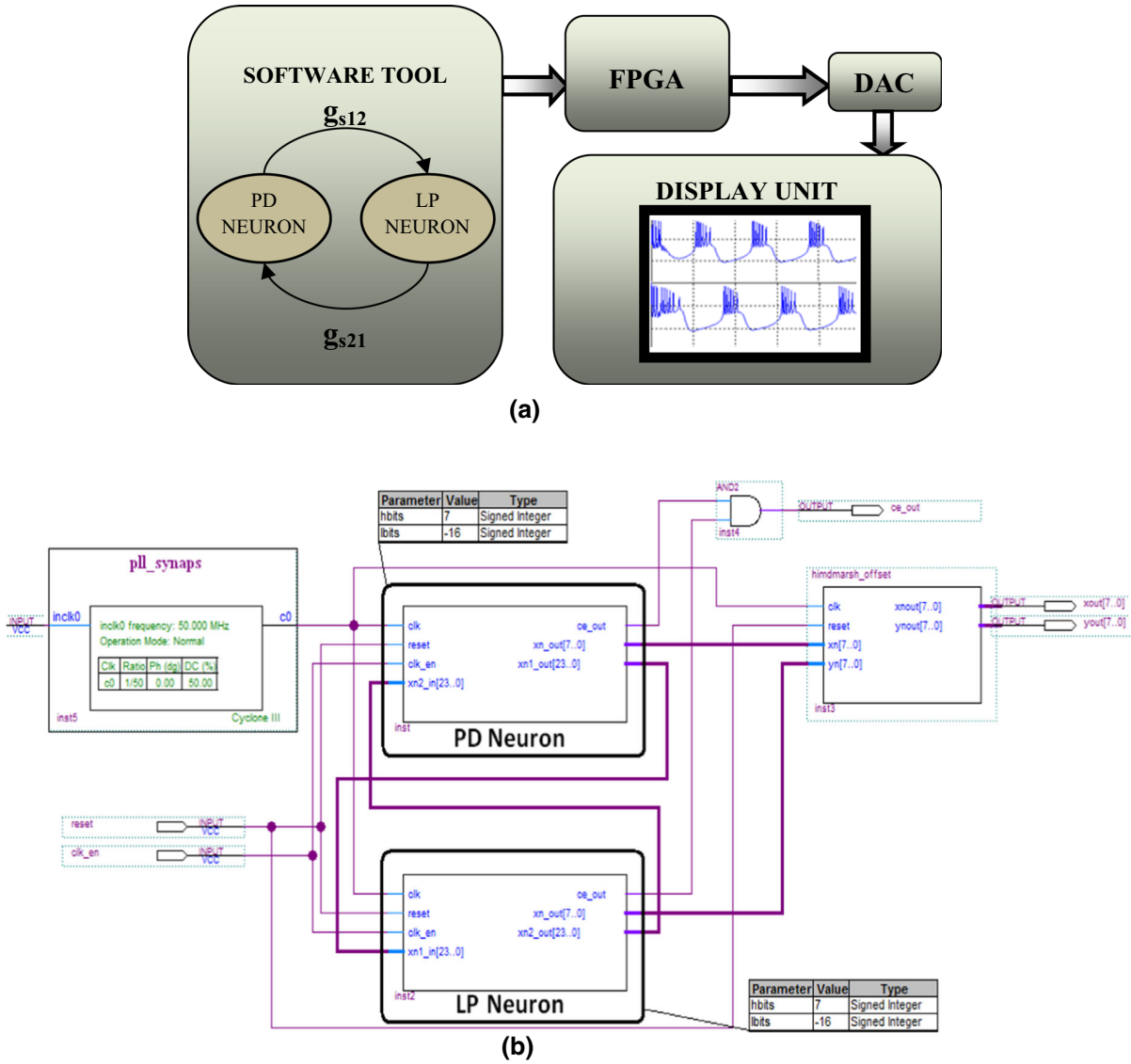

Fig. 9 **a** Schematic block diagram for FPGA-based implementation of chemical coupled two HR neurons, **b** VHDL design schemes on Quartus II software of the chemical coupled HR neurons

modified function, electrical coupling is a better choice for digital devices-based implementations.

4 Conclusions

In this study, versatile implementations of the chemical coupled two HR neurons are performed with programmable analog and digital devices successfully. The interactions of the collective neurons are emulated with analog programmable device precisely. Since nonlinear chemical coupling function is hard to realize with digital devices, it has been concentrated on the digital implementation of this function. The digital device-based implementation difficulty problem of the nonlinear chemical coupling function is solved by modifying this coupling function.

After the rescaling and the CAM blocks selection process, construction of the required connections between the CAM blocks are done by using the FPAA interface tool to build analog programmable devices-based HR neurons. Thus, program-

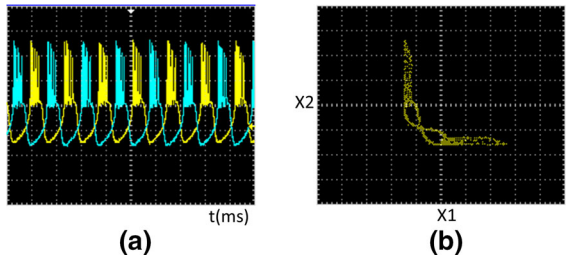

Fig. 10 FPGA-based experimental results of the chemical coupled two HR neurons **a** x_1, x_2 time domain illustrations, x, 500 mV/div; y, 500 mV/div; time/div, 10 ms. **b** x-y phase portrait illustration of x_1 and x_2 x, 500 mV/div; y, 500 mV/div for asynchronous behavior

mable analog device-based realization of the chemical coupled HR neurons is reported in this study on the crest of a wave. Although CAB usage capacities and power consumptions increase just a little, four FPAA boards are used for the realization of the chemical coupled HR neurons like as the electrical one.

In the programmable digital device-based implementation process of the chemical coupled HR neurons, firstly, the chemical coupling function is transformed to an approximate nonlinear function in order to overcome the digital device implementation difficulty. Then, the stability control of the new modified chemical coupling function is checked by using the standard deviation method and the synchronization statuses of modified chemical coupled HR neurons are adjusted by utilizing the result of standard deviation method. Therefore, the modified chemical coupled two HR neurons are implemented with FPGA as an example of digital realization for the first time in literature. When the synthesis results of FPGA-based realizations of the electrically and chemically coupled HR neurons are compared with each other, the maximum operating frequency, the area consumption and the number of the used bit of the chemical coupled HR neurons become worse. However, digital implementation deficiency problem of the chemical coupled HR neurons is alleviated by using this modified function.

According to these results, both of the programmable and reconfigurable devices have been used effectively in the experimental realization of the chemical coupled HR neurons. However, there are several advantages of each of these analog and digital reconfigurable devices in terms of the design methodologies. While one FPGA board was sufficient for FPGA implementations in terms of capacity usage, four FPAA boards were required for FPAA implementations. The power consumption of FPAA is more than the FPGA, because of the usage multiple boards in the FPAA-based implementation. On the other hand, the outputs of the FPGA were obtained through DACs and the performance of the FPGA remained dependent on the bit resolution of the DAC in use. In contrast, there was no requirement for an external device to observe the neural dynamics for FPAA. While the nonlinear expression in the chemical coupling function is implemented with FPAA without the need for any extra process, an approximate nonlinear function is used in the digital reconfigurable device implementation. Additionally, although devices performances of the FPGA become worse, digital platform implementation presented closer behaviors to simulation results. Despite of these shortcomings of the reconfigurable platforms, the neuronal realization studies in here may lead to other CPG circuit implementations. It is seen that hardware solutions depending on analog and digital programmable devices play effective roles in various CPG circuit applications. By using design techniques presented here, prototypes of other neuronal applications can be constructed rapidly and the testing and verifying process can be executed on these programmable platforms. After the realization of the chemical coupling function with these useful reconfigurable analog and digital platforms in this study, a whole CPG network structure can be constructed with these experimental platforms consummately in the future work studies.

Table 2 Synthesis results and estimated power consumptions of the FPGA-based implementation

	Area usage (logic elements) (%)	Embedded multiplier usage (%)	Maximum frequency (MHz)	Bit length
Electrical coupling [61]	4851 (31)	104 (93)	14.19	32
Chemical coupling	8925 (58)	96 (86)	3.54	24

References

1. Pecora, L.M., Carroll, T.L.: Synchronization in chaotic systems. Phys. Rev. Lett. **64**, 821–824 (1990)
2. Kocarev, L., Parlitz, U.: General approach for chaotic synchronization with applications to communication. Phys. Rev. Lett. **74**, 5028–5031 (1995)
3. Terry, J.R., Thornburg, K.S., De Shazer, D.J., Van Wiggeren, G.D., Zhu, S.Q., Ashwin, P., Roy, R.: Synchronization of chaos in an array of three lasers. Phys. Rev. E **59**, 4036–4043 (1999)
4. Yang, X.S., Cao, J.D.: Finite-time stochastic synchronization of complex networks. Appl. Math. Model. **34**, 3631–3641 (2010)
5. Gray, C.M., König, P., Engel, A.K., Singer, W.: Oscillatory responses in cat visual cortex exhibit inter-columnar synchronization with reflects global stimulus properties. Nature **338**, 334–337 (1989)
6. Kreiter, A.K., Singer, W.: Stimulus-dependent synchronization of neuronal responses in the visual cortex of the awake macaque monkey. J. Neurosci. **16**, 2381–2396 (1996)
7. Roelfsema, P.R., Engel, A.K., König, P., Singer, W.: Visuomotor integration is associated with zero time-lag synchronization among cortical areas. Nature **385**, 157–161 (1997)
8. Hodgkin, A., Huxley, A.: A quantitative description of membrane current and its application to conduction and excitation in nerve. J. Phisiol. (Lond) **117**, 500–544 (1952)
9. FitzHugh, R.: Mathematical models for excitation and propagation in nerve. In: Schawn, H.P. (ed.) Biological Engineering, vol. 1, pp. 1–85. McGraw-Hill, New York (1969)
10. Wilson, H.R., Cowan, J.D.: Excitatory and inhibitory interactions in localized populations of model neurons. Biophys. J. **12**(1), 1–24 (1972)
11. Morris, C., Lecar, H.: Voltage oscillations in the barnacle giant muscle fiber. Biophys. J. **35**, 193–213 (1981)
12. Hindmarsh, J.L., Rose, R.M.: A model of neural bursting using three couple first order differential equations. Proc. R. Soc. Lond. Biol. Sci. **221**(1222), 87–102 (1984)
13. Izhikevich, E.M.: Simple model of spiking neurons. IEEE Trans. Neural Netw. **14**(6), 1569–1572 (2003)
14. Kandel, E.R., Schwartz, J.H., Jessell, T.M.: Principles of Neural Science, 4th ed. McGraw-Hill, New York. ISBN 0-8385-7701-6 (2000)
15. Miller, J.P., Selverston, A.I.: Mechanisms underlying pattern generation in lobster stomatogastric ganglion as determined by selective inactivation of identified neurons. II. Oscillatory properties of pyloric neurons. J. Neurophysiol. **48**(6), 1378–1391 (1982)
16. Li, C.H., Yang, S.Y.: Effects of network structure on the synchronizability of nonlinearly coupled Hindmarsh-Rose neurons. Phys. Lett. A **379**, 2541–2548 (2015)
17. Hrg, D.: Synchronization of two Hindmarsh–Rose neurons with unidirectional coupling. Neural Netw. **40**, 73–79 (2013)
18. Jhou, F.J., Juang, J., Liang, Y.H.: Multistate and multistage synchronization of Hindmarsh–Rose neurons with excitatory chemical and electrical synapses. IEEE Trans. Circuits Syst. I Regul. Pap. **59**(6), 1335–1347 (2012)
19. Wei, W.: Synchronization of coupled chaotic Hindmarsh Rose neurons: an adaptive approach. Chin. Phys. B **24**(10), 100503 (2015)
20. Nguyen, L.H., Hong, K.S.: Adaptive synchronization of two coupled chaotic Hindmarsh–Rose neurons by controlling the membrane potential of a slave neuron. Appl. Math. Model. **37**, 2460–2468 (2013)
21. Nguyen, L.H., Hong, K.S.: Synchronization of coupled chaotic FitzHugh–Nagumo neurons via Lyapunov functions. Math. Comput. Simul. **82**, 590–603 (2011)
22. Rehan, M., Hong, K.S., Aqil, M.: Synchronization of multiple chaotic FitzHugh–Nagumo neurons with gap junctions under external electrical stimulation. Neurocomputing **74**, 3296–3304 (2011)
23. Aqil, M., Hong, K.S., Jeong, M.Y.: Synchronization of coupled chaotic FitzHugh–Nagumo systems. Commun. Nonlinear Sci. Numer. Simul. **17**, 1615–1627 (2012)
24. Deng, B., Wang, J., Fei, X.: Synchronizing two coupled chaotic neurons in external electrical stimulation using backstepping control. Chaos Solitons Fractals **29**, 182–189 (2006)
25. Sun, L., Wang, J., Deng, B.: Global synchronization of two Ghostburster neurons via active control. Chaos Solitons Fractals **40**, 1213–1220 (2009)
26. Wang, J., Chen, L.S., Deng, B.: Synchronization of Ghostburster neuron in external electrical stimulation via H-infinity variable universe fuzzy adaptive control. Chaos Solitons Fractals **39**, 2076–2085 (2009)
27. Aguilar-Lópex, R., Martínez-Guerra, R.: Synchronization of coupled Hodgkin–Huxley neurons via high order sliding-mode feedback. Chaos Solitons Fractals **37**, 539–546 (2008)
28. Che, Y.Q., Wang, J., Tsang, K.M., Chan, W.L.: Unidirectional synchronization for Hindmarsh–Rose neurons via robust adaptive sliding mode control. Nonlinear Anal. Real World Appl. **11**, 1096–1104 (2010)
29. Dtchetgnia Djeundam, S.R., Yamapi, R., Filatrella, G., Kofane, T.C.: Stability of the synchronized network of Hindmarsh–Rose neuronal models with nearest and global couplings. Commun. Nonlinear Sci. Numer.Simul. **22**, 545–563 (2015)
30. Wang, C., He, Y., Ma, J., Huang, L.: Parameters estimation, mixed synchronization, and antisynchronization in chaotic systems. Complexity **20**(1), 64–73 (2014)
31. Zhang, J.Q., Huang, S.F., Pang, S.T., Wang, M.S., Gao, S.: Synchronization in the uncoupled neuron system. Chin. Phys. Lett. **32**(12), 9–13 (2015)
32. Li, C.H., Yang, S.Y.: Eventual dissipativeness and synchronization of nonlinearly coupled dynamical network of Hindmarsh–Rose neurons. Appl. Math. Model. **39**, 6631–6644 (2015)
33. Pecora, L.M., Carroll, T.L.: Master stability functions for synchronized coupled systems. Int. J. Bifurc. Chaos **80**, 2109–2112 (1998)
34. Belykh, V., Belykh, I., Hasler, M.: Connection graph stability method for synchronized coupled chaotic systems. Phys. D Nonlinear Phenom. **195**, 159–187 (2004)
35. Belykh, I., Belykh, V., Hasler, M.: Synchronization in asymmetrically coupled networks with node balance. Chaos Interdiscip. J. Nonlinear Sci. **16**, 015102 (2006)
36. Belykh, I., Belykh, V., Hasler, M.: Generalized connection graph method for synchronization in asymmetrical networks. Phys. D Nonlinear Phenom. **224**, 42–51 (2006)

37. Chen, T., Zhu, Z.: Exponential synchronization of nonlinear coupled dynamical networks. Int. J. Bifurc. Chaos **17**, 999–1005 (2007)
38. Liu, X., Chen, T.: Synchronization analysis for nonlinearly-coupled complex networks with an asymmetrical coupling matrix. Phys. A Stat. Mech. Appl. **387**, 4429–4439 (2008)
39. Lu, W., Chen, T.: New approach to synchronization analysis of linearly coupled ordinary differential systems. Phys. D Nonlinear Phenom. **213**, 214–230 (2006)
40. Liu, X., Chen, T.: Boundedness and synchronization of y-coupled Lorenz systems with or without controllers. Phys. D Nonlinear Phenom. **237**, 630–639 (2008)
41. Chen, M.: Synchronization in time-varying networks: a matrix measure approach. Phys. Rev. E **76**, 016104 (2007)
42. Juang, J., Li, C.-L., Liang, Y.-H.: Global synchronization in lattices of coupled chaotic systems. Chaos Interdiscip. J. Nonlinear Sci. **17**, 033111 (2007)
43. Baptista, M.S., Moukam Kakmeni, F.M., Grebogi, C.: Combined effect of chemical and electrical synapses in Hindmarsh–Rose neural networks on synchronization and the rate of information. Phys. Rev. E **82**, 036203 (2010)
44. Li, Z.: Exponential stability of synchronization in asymmetrically coupled dynamical networks. Chaos Interdiscip. J. Nonlinear Sci. **18**(2), 023124 (2008)
45. Li, Z., Lee, J.: New eigenvalue based approach to synchronization in asymmetrically coupled networks. Chaos Interdiscip. J. Nonlinear Sci. **17**(4), 043117 (2007)
46. Checco, P., Righero, M., Biey, M., Kocerev, L.: Information processing in networks of coupled Hindmarsh–Rose neurons. In: International Symposium on Nonlinear Theory and its Applications Bologna-Italy, NOLTA, pp. 671–674 (2006)
47. Gu, H., Pan, B., Chen, G., Duan, L.: Biological experimental demonstration of bifurcations frombursting to spiking predicted by theoretical models. Nonlinear Dyn. **78**, 391–407 (2014)
48. Abarbanel, H.D.I., Rabinovich, M.I., Selverston, A., Bazhenov, M.V., Huerta, R., Sushchik, M.M., Rubchinskii, L.L.: Synchronization in neural networks. Phys. Uspekhi **39**(4), 337–362 (1996)
49. Elson, R.C., Selverston, A.I., Huerta, R., Rulkov, N.F., Rabinovich, A.I., Abarbanel, H.D.I.: Synchronous behavior of two coupled biological neurons. Phys. Rev. Lett. **81**(25), 5692–5695 (1998)
50. Hizanidis, J., Kanas, V., Bezerianos, A., Bountis, T.: Chimera states in networks of nonlocally coupled Hindmarsh–Rose neuron models. Int. J. Bifurc. Chaos **24**(3), 1450030 (2014)
51. Lu, J., Yang, J., Kim, Y.B., Ayers, J., Kim, K.K.: Implementation of excitatory CMOS neuron oscillator for robot motion control unit. J. Semiconduct. Technol. Sci. **14**(4), 383–390 (2014)
52. Charles, G., Gordon, C., Alexander, W.E.: An implementation of a biological neural model using analog-digital integrated circuits. In: IEEE International Behavioral Modeling and Simulation Workshop, BMAS, pp. 78–83 (2008)
53. Pinto, R.D., Varona, P., Volkovskii, A.R., Szücs, A., Abarbanel, H.D.I., Rabinovich, M.I.: Synchronous behavior of two coupled electronic neurons. Phys. Rev. E **62**(2000), 2644–2656 (2000)
54. Merlat, L., Silvestre, N., Merckle, J.: A Hindmarsh and Rose-based electronic burster. In: Proceedings of Fifth International Conference on Microelectronics for Neural Networks, pp. 39-44 (1996)
55. Poggi, T., Sciutto, A., Storace, M.: Piecewise linear implementation of nonlinear dynamical systems: from theory to practice. Electron. Lett. **45**(19), 966–967 (2009)
56. Gotthans, T., Petrzela, J., Hrubos, Z.: Analysis of Hindmarsh–Rose neuron model and novel circuitry realization. In: Proceedings of the 18th International Conference Mixed Design of Integrated Circuits and Systems (MIXDES), pp. 576–580 (2011)
57. Linaro, D., Poggi, T., Storace, M.: Experimental bifurcation diagram of a circuit-implemented neuron model. Phys. Lett. A **374**, 4589–4593 (2010)
58. Korkmaz, N., Öztürk, İ., Kiliç, R.: Multiple perspectives on the hardware implementations of biological neuron models and programmable design aspects. Turk. J. Electr. Eng. Comput. Sci. **24**(3), 1729–1746 (2016)
59. Steur, E.: On synchronization of electromechanical Hindmarsh–Rose Oscillators. Eindhoven University of Technology, Master Thesis (2007)
60. Jacquir, S., Binczak, S., Bilbault, J.M., Kazantsev, V., Nekorkin, V.: Synaptic coupling between two electronic neurons. Nonlinear Dyn. **44**, 29–36 (2006)
61. Dahasert, N., Öztürk, İ., Kiliç, R.: Experimental realizations of the HR neuron model with programmable hardware and synchronization applications. Nonlinear Dyn. **70**(4), 2343–2358 (2012)
62. Song, X., Wang, C., Ma, J., Tang, J.: Transition of electric activity of neurons induced by chemical and electric autapses. Sci. China Technol. Sci. **58**(6), 1007–1014 (2015)
63. Wu, X., Ma, J., Yuan, L., Liu, Y.: Simulating electric activities of neurons by using PSPICE. Nonlinear Dyn. **75**(1), 113–126 (2014)
64. Ma, J., Tang, J.: A review for dynamics of collective behaviors of network of neurons. Sci. China Technol. Sci. **58**, 2038–2045 (2015)
65. Yang, S., Wang, J., Li, S., Deng, B., Wei, X., Yu, H., Li, H.: Cost-efficient FPGA implementation of basal ganglia and their Parkinsonian analysis. Neural Netw. **71**, 62–75 (2015)
66. Marder, E., Calabrese, R.L.: Principles of rhythmic motor pattern generation. Phys. Rev. **76**(3), 687–717 (1996)
67. Ijspeert, A.J.: Central pattern generators for locomotion control in animals and robots: a review. Neural Netw. **21**, 642–653 (2008)
68. www.anadigm.com
69. www.altera.com